ATP-release pannexin channels are gated by lysophospholipids

Erik Henze[1]†, Jacqueline J. Ehrlich[1]†, Russell N. Burkhardt[2], Bennett W. Fox[2], Kevin Michalski[1]‡, Lydia Kramer[1]§, Margret Lenfest[3], Jordyn M. Boesch[3], Frank C. Schroeder[2], and Toshimitsu Kawate[1]*

[1]Department of Molecular Medicine, Cornell University, Ithaca, NY 14853, USA

[2]Boyce Thompson Institute and Department of Chemistry and Chemical Biology, Cornell University, Ithaca, NY 14853, USA

[3]Department of Clinical Sciences, College of Veterinary Medicine, Cornell University, Ithaca, NY 14853, USA

*Corresponding author. Email: toshi.kawate@cornell.edu

†These authors contributed equally to this work.

‡Present address: WM Keck Structural Biology Laboratory, Cold Spring Harbor Laboratory, Cold Spring Harbor, NY 11724, USA

§Present address: Department of Pharmacology and Molecular Sciences, Johns Hopkins University School of Medicine, Baltimore, MD 21205, USA

Abstract: Adenosine triphosphate (ATP) serves as an extracellular messenger that mediates diverse cell-to-cell communication. Compelling evidence supports that ATP is released from cells through pannexins, a family of heptameric large pore-forming channels. However, the activation mechanisms that trigger ATP release by pannexins remain poorly understood. Here, we discover lysophospholipids as endogenous pannexin activators, using activity-guided fractionation of mouse tissue extracts combined with untargeted metabolomics and electrophysiology. We show that lysophospholipids directly and reversibly activate pannexins in the absence of other proteins. Molecular docking, mutagenesis, and single-particle cryo-EM reconstructions suggest that lysophospholipids open pannexin channels by altering the conformation of the N-terminal domain. Our results provide a connection between lipid metabolism and ATP signaling, both of which play major roles in inflammation and neurotransmission.

One-Sentence Summary: Untargeted metabolomics discovers a class of messenger lipids as endogenous activators of membrane channels important for inflammation and neurotransmission.

Main Text: Purine nucleotides are essential building blocks for DNA and RNA and for fueling cellular processes. But purine nucleotides, most prominently adenosine triphosphate (ATP), also mediate cell-to-cell communication as extracellular signal transmitters (*1*). Such "purinergic signaling" orchestrates important physiological events throughout the body (*2, 3*), controlling the senses of taste (*4*) and sight (*5*), the sensation of pain (*6*), and the activation of white blood cells (*7*). Because of its vast reach, the receptors and hydrolyzing enzymes for extracellular ATP are emerging drug targets for many hard-to-cure diseases, such as arthritis and chronic cough (*8, 9*). However, the mechanism by which ATP is released from cells remains poorly understood.

Pannexins, a unique family of heptameric large pore-forming membrane channels, have been shown to release signaling molecules like ATP from both dying and living cells (*10, 11*). Pannexin-mediated ATP release from dying cells is important not only for depleting cellular energy and halting metabolism, but also for facilitating the recruitment of white blood cells (*12, 13*). This so-called "find me" signaling allows macrophages and neutrophils to clear billions of dying cells daily without causing inflammation. Single channel recordings and *in vitro* reconstitution studies demonstrated that cleavage of the C-terminus by caspase during apoptotic cell death triggers pannexin1 (Panx1) channel opening (*14, 15*). To explain this mode of activation, a simple pore blocking/unblocking has been proposed; if the C-terminus plugs the pore, cleavage of this region will unplug the pore (*16*). However, the actual mechanism appears more complex, as a Panx1 construct lacking the C-terminus can be closed (*17, 18*). Further, this irreversible mode of activation occurs only in dying cells, which cannot explain the many signaling roles pannexins play in living cells, such as immune cell migration and differentiation, epileptic seizures, migraine, and chronic pain (*19-22*). Pannexins are also implicated in other common health problems, such as obesity (*23, 24*) and hypertension (*25*).

In living cells, studies have suggested that Panx1 is activated through intracellular signaling triggered by the stimulation of structurally unrelated membrane receptors, such as G protein-coupled receptors (e.g., α1-adrenergic receptor (*26*)), ligand-gated ion channels (e.g., NMDA receptor (*27*)), and tumor necrosis factor receptors (*28*). Multiple post-translational modifications, such as phosphorylation and acetylation, have been proposed to control Panx1 channel activity (*29, 30*), but the problem here is speed; it is questionable whether such enzyme-dependent mechanisms can work on a milliseconds to seconds time scale to transiently open and close a membrane pore permeable to a large cell metabolite like ATP. Other miscellaneous stimuli, such as high concentrations of extracellular K^+, membrane stretch, and membrane depolarization, have also been demonstrated to activate Panx1 (*31*). However, it remains unclear how these apparently unrelated stimuli can activate Panx1, despite the available cryo-EM structures (*18, 32-35*). Essentially nothing is known about the activation mechanisms of other subtypes (i.e., Panx2 and Panx3). To shed new light on the mechanisms of pannexin activation in living cells, we searched for a *bona fide* and reversible stimulus.

Panx1 and Panx2 are activated by lysophospholipids

Our previous studies demonstrated that a small molecule, such as probenecid, could reversibly activate a point mutant of Panx1 (e.g., W74A)(*36*). We hypothesized that naturally occurring small molecules could trigger pannexin channel opening. To identify the gating molecules, we used an activity-guided fractionation approach (*37*). Mouse liver extract was fractionated using reverse-phase chromatography and the fractions were tested for Panx1 and Panx2 activation using whole-cell patch-clamp electrophysiology (Fig. 1A). We employed a construct that contains a Gly-Ser insertion at the N-terminus (dubbed "Panx1+GS"), which yields significantly larger currents than the wild type channel in HEK293 cells (*38*). We excluded Panx3 from the screening because it failed to activate even at an extreme membrane potential (> +100 mV), despite detectable surface expression in mammalian tissue culture cells (Fig. S1A). Among the 18

fractions, two fractions (#11 and #12) gave rise to robust and reversible currents specific to Panx1+GS or Panx2 (Fig. S2A, B, and F). Comparative analysis by high performance liquid chromatography coupled to high-resolution mass spectrometry (HPLC-HRMS) revealed approximately 1,500 features that were enriched more than 10-fold in active fractions compared to neighboring fractions, which showed negligible activity. To reduce the number of candidate metabolites, we pooled the active fractions and performed another round of activity-guided fractionation. One of the resulting fractions (# 7) strongly activated both Panx1+GS and Panx2 (Fig. S2C-E and G). Comparative metabolomic analysis revealed two major metabolites significantly enriched in this fraction: lysophosphatidylcholine (LPC)-16:0 (Fig. 1B and C) and LPC-22:5. LPCs exist in extracellular fluids at high micromolar concentrations and play diverse signaling roles, especially in inflammation (*39*).

To test whether LPCs activate pannexins, we performed whole-cell patch-clamp recordings using synthetic compounds. We focused on LPC16:0, which is readily available and found to be the most abundant LPC variants in extracellular fluids (*40*). A robust and reversible current was observed for both Panx1+GS and Panx2 (Fig. 1D and E and Fig. S1B), while Panx3 and other large-pore channels, including LRRC8A, connexin 43, and innexin 6, failed to show measurable currents under the same experimental conditions (Fig. 1D and E, and Fig. S1B and C). Recordings from vector-transfected cells and carbenoxolone (CBX) sensitivity confirmed that the LPC16:0-mediated currents were specific to pannexins (Panx2 is insensitive to CBX)(*41*). The wildtype Panx1 also robustly responded to LPC16:0 when it was expressed in HEK293S GnTI$^-$ cells, an HEK derivative commonly used for structural studies (*42*)(Fig. 1D and E). Interestingly, LPC16:0 activated Panx2 in both cell types, while adding Gly and Ser at the N-terminus abolished its channel activity (Fig. 1D and Fig. S1C and 3G). These data suggest that the pannexin N-terminus plays a prominent role in channel regulation and that cell-dependent mechanisms involving this region may "prime" Panx1 for its activation. Importantly, extracellular ATP levels significantly increased when Panx1- or Panx2-expressing cells were stimulated with LPC16:0 (Fig. 1F). These results corroborate that LPC16:0 is a signaling metabolite that promotes ATP release from living cells through activation of Panx1 and/or Panx2.

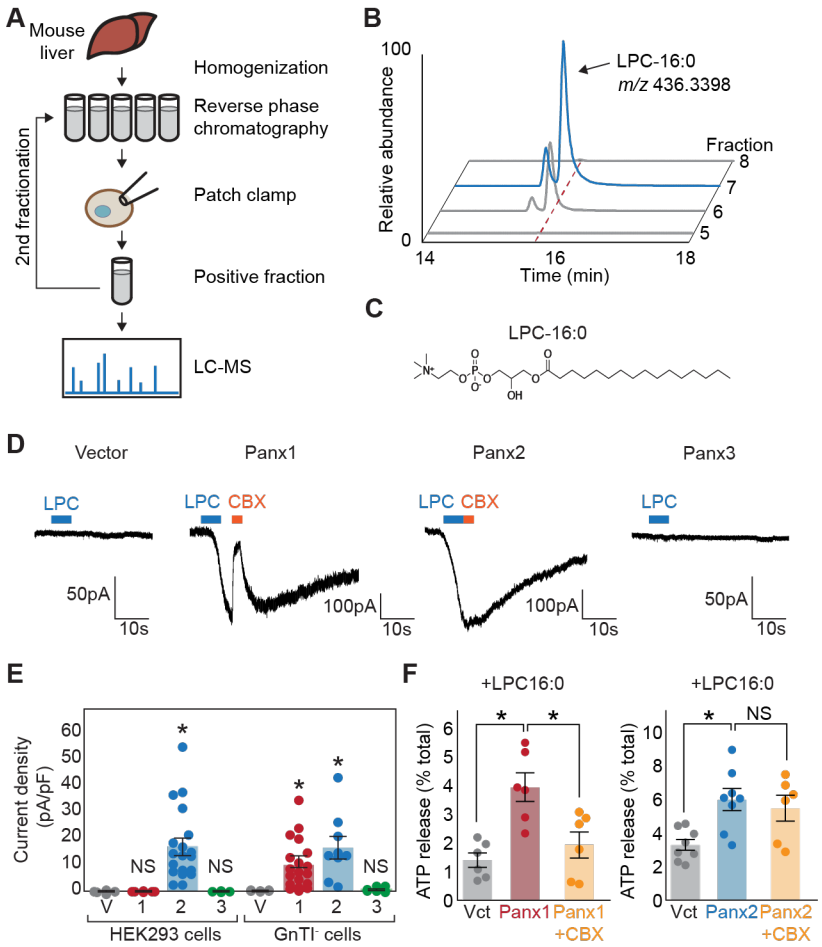

Fig. 1. Metabolomic screening identifies LPC-16:0 as a pannexin agonist. (**A**) Schematic of screening process. Organic extracts of mouse liver tissues were subjected to polarity-based fractionation and assessed for their ability to stimulate currents in HEK cells expressing Panx1+GS or Panx2 using whole-cell patch-clamp. Active fractions were analyzed by liquid chromatography–mass spectrometry. (**B**) LC-MS traces for fractions #5-8 from the second round of Panx1+GS activity-guided fractionation. (**C**) Chemical structure of LPC-16:0. (**D**) and (**E**) Representative whole-cell patch-clamp traces (D) and quantification of peak current densities (E) triggered by LPC-16:0. Panx1 (wildtype) was expressed in GnTI$^-$ cells while the other constructs were expressed in HEK cells. Voltage-clamp recordings were performed at -60 mV. Blue bars indicate application of LPC-16:0 (7 μM), and orange bars indicate application of carbenoxolone (50 μM). n=5-20. One-way ANOVA followed by Dunnett's test was used to assess statistical significance. (**F**) ATP release induced by application of LPC-16:0 (10 μM) to Panx1-expressing GnTI$^-$ (left) and Panx2-expressing HEK (right) cells. Data are expressed as percent of total ATP released upon membrane solubilization. n=6-8. P values were calculated using unpaired t-test with unequal variances. An asterisk denotes $p<0.01$ for all tests. Error bars represent s.e.m.

We next tested structurally diverse lysophospholipids for pannexin activity. To facilitate high-throughput screening of multiple chemicals, we developed a fluorescence-based assay where anion influx through pannexin is measured by following fluorescence quenching of a halide biosensor "mVenus" (Fig. 2A)(*43, 44*). We found that applying LPC16:0 robustly quenched mVenus fluorescence in cells expressing Panx1 and 2 (Fig. 2B-E). Likewise, LPCs with 14:0, 18:0, 2-16:0, or 18:1 acyl groups activated both Panx1 and 2 with similar estimated EC50 values

within the 10-50 μM range (Fig. 2F and G, Fig. S3). In contrast, neither LPC12:0 nor LPC20:0 activated these pannexins, suggesting that the most effective LPC chain length is between 14 and 18 carbons. Lysophospholipids with other headgroups, including lysophosphatidic acid (LPA), lysophosphatidylinositol (LPI), and sphingosylphosphorylcholine (SPC) were as potent as LPC, whereas lysophosphatidylethanolamine (LPE) failed to activate pannexins even at 100 μM (Fig. S3). Together, these results suggest that pannexins are activated by select lysophospholipids, but the ones that activate pannexins share similar potencies. Considering that the extracellular concentrations of LPCs are orders of magnitude higher than the other tested species (*40*), Panx1 and Panx2 are most likely activated by LPCs in the body.

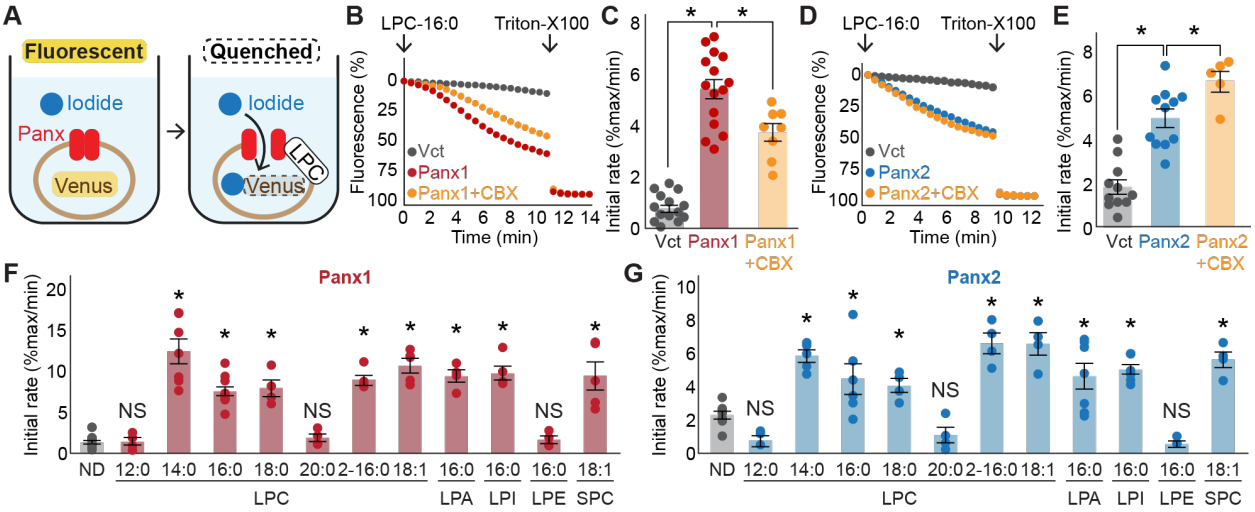

Fig. 2: Cellular mVenus-quench assay reveals a family of lysophospholipids as pannexin agonists. (**A**) Cartoon illustrating the principle of the mVenus quench assay. (**B**)-(**E**) Representative traces ((B) for Panx1 and (D) for Panx2) and quantification of initial mVenus quenching rates ((C) for Panx1 and (E) for Panx2). LPC-16:0 (30 μM) was applied with or without CBX (50 μM), and the maximum mVenus quenching was measured after cell solubilization with 1% Triton-X100. n=8-14. P values were calculated using unpaired t-test with unequal variances. (**F**) and (**G**) Initial mVenus quenching rates of Panx1 expressed in GnTI$^-$ cells (F) and Panx2 expressed in HEK cells (G). Pannexin activation was induced by 60 μM of saturated sn-1 LPCs (LPC-12:0-20:0), sn-2 LPC (LPC2-16:0), a monounsaturated sn-1 (LPC-18:1), or other sn-1 lysophospholipids with different headgroups (LPA-16:0, LPI-16:0, LPE-16:0, and SPC-18:1). n=4-14 for all conditions. P values were calculated using one-way ANOVA followed by Dunnett's t-test. Asterisks denote p<0.01. Error bars represent s.e.m.

Lysophospholipids directly activate Panx1

Studies suggest that several ion channels and membrane receptors are activated by lysophospholipids (*40, 45, 46*). To test whether lysophospholipids directly activate pannexins, we performed a functional reconstitution where pannexin activity can be studied in the absence of other proteins (Fig. 3A). The full-length Panx1 was tagged in the flexible internal loop to preserve the native N- and C-terminal domains that likely play key roles in channel gating (Fig. 3B). We used GnTI$^-$ cells for protein expression because Panx1 is robustly activated by LPC16:0 in these cells. Purified Panx1 (Fig. S4A and B) was reconstituted into proteoliposomes composed of 1-palmitoyl-2-oleoyl-sn-glycero-3-phosphoethanolamine (POPE), 1-palmitoyl-2-oleoyl-sn-glycero-3-phosphoglycerol (POPG), and sphingomyelin (SM; brain extract). We then measured YO-PRO-1 dye uptake, a widely used assay for probing Panx1 channel activity (*47*). We confirmed that

LPC16:0 triggers YO-PRO-1 uptake in Panx1-expressing GnTI$^-$ cells using a cell-based assay (Fig. S4C). Upon LPC16:0 application, Panx1-reconstituted proteoliposomes took up YO-PRO-1 in a dose-dependent manner (Fig. 3C and D). Control experiments with empty and CBX-treated liposomes confirmed that the observed YO-PRO-1 uptake was Panx1 dependent. These results provide evidence that lysophospholipids directly activate Panx1 in the absence of other proteins.

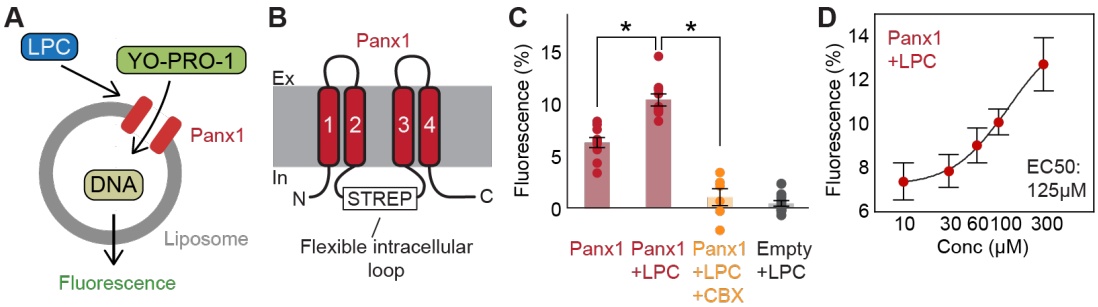

Fig. 3: Functional reconstitution of Panx1 confirms direct activation by LPC16:0. (**A**) Schematic representation of YO-PRO-1 uptake assay. (**B**) A schematic representation of the full length Panx1 construct used for functional reconstitution. Gray area: plasma membrane; Ex: extracellular; In: intracellular. (**C**) Relative YO-PRO-1 fluorescence triggered by LPC16:0 (100 μM) with or without CBX (50 μM). Asterisks indicate $p < 0.01$ using a unpaired t-test. n=6-15. (**D**) Dose-response profile of Panx1 treated with LPC-16:0. Dose responses were fitted with the Hill equation, and the EC50 values are indicated. n=10-13. Error bars represent s.e.m.

Phospholipase A mediates pannexin activation

Lysophospholipids are produced from membrane phospholipids through catalytic action mediated primarily by phospholipase A1 (PLA1) or A2 (PLA2) (*40*). PLA1 hydrolyzes phospholipids and produces 2-acyl-1-lysophospholipids and free fatty acids that play pivotal roles in many important life processes, such as inflammation (Fig. 4A)(*48*). Likewise, Multiple classes of PLA2 enzymes exist both inside and outside of cells and hydrolyze phospholipids into lysophospholipids and free fatty acids. Considering that extracellular ATP concentration increases during inflammation (*49*), we wondered whether phospholipase A activation may lead to pannexin channel opening. To test this possibility, we first assessed whether extracellular application of PLA1 or sPLA2, a secreted form of this enzyme, can open pannexin channels. As with LPC16:0, we found that application of PLA1 or sPLA2 resulted in robust mVenus quenching for both Panx1- and Panx2-expressing cells (Fig. 4B and C). Since PLA2 also leads to the production of signaling molecules other than lysophospholipids, we also tested several representative lipid metabolites known to mediate inflammatory responses (*50*). However, none of the tested lipid species, namely arachidonic acid, N-arachidonoylethanolamine, prostaglandin E2, and prostaglandin I2, triggered mVenus quenching (Fig. 4D). These results suggest that lysophospholipids, but not free fatty acids, generated from the plasma membrane can activate pannexins.

We next tested whether endogenously existing cytoplasmic PLA2 (e.g., cPLA2) can activate pannexins. PLA2 is activated by polycationic amphipathic peptides commonly found in the venom of poisonous creatures. One such peptide is mastoparan, a toxic component of wasp venom that can induce cPLA2 activity in a variety of cell types (*51, 52*). Indeed, application of mastoparan caused a robust, CBX-sensitive mVenus quenching in cells expressing Panx1 (Fig. 4E). This quenching was attenuated by the PLA2 inhibitors chlorpromazine (CPZ) and quercetin (QCT). Because mastoparan application may trigger Panx1 activation through other mechanisms, such as C-terminal cleavage by caspase or activation of Src kinases, we applied mastoparan following preincubation with a pan-caspase inhibitor Z-DEVD-FMK or the Src inhibitor

PP2. However, neither inhibitor affected mastoparan-dependent mVenus quenching, indicating that indirect modes of Panx1 activation were unlikely (Fig. 4E). Interestingly, mastoparan-mediated mVenus quenching was not observed in cells expressing Panx2. It is possible that Panx2 may prefer lysophospholipids produced from the outer membrane leaflet. Together, these experiments indicate that both PLA1 and PLA2 can activate pannexins, likely through the production of lysophospholipids from the plasma membrane.

Synovial fluid from canine patients experiencing pain stimulates Panx1

Given that lysophospholipid and phospholipase concentrations are elevated in patients suffering from joint diseases (*53*), we hypothesized that synovial fluids from dogs with naturally occurring algogenic disease might trigger Panx1 activation. To test this hypothesis, we collected joint fluid from 22 canine patients, which were behaviorally assessed to be suffering from varying degrees of pain, and measured Panx1 channel activity using the mVenus cell-based assay. We found that the joint fluid collected from patients with moderate to severe pain triggered a robust mVenus quenching (Fig. 4F). In contrast, joint fluid collected from patients assessed to have only mild pain showed significantly weaker mVenus quenching. These data demonstrate that such joint fluid contains signaling metabolites—likely lysophospholipids, based on the current study—that can activate Panx1 in the presence of other molecules in extracellular fluids.

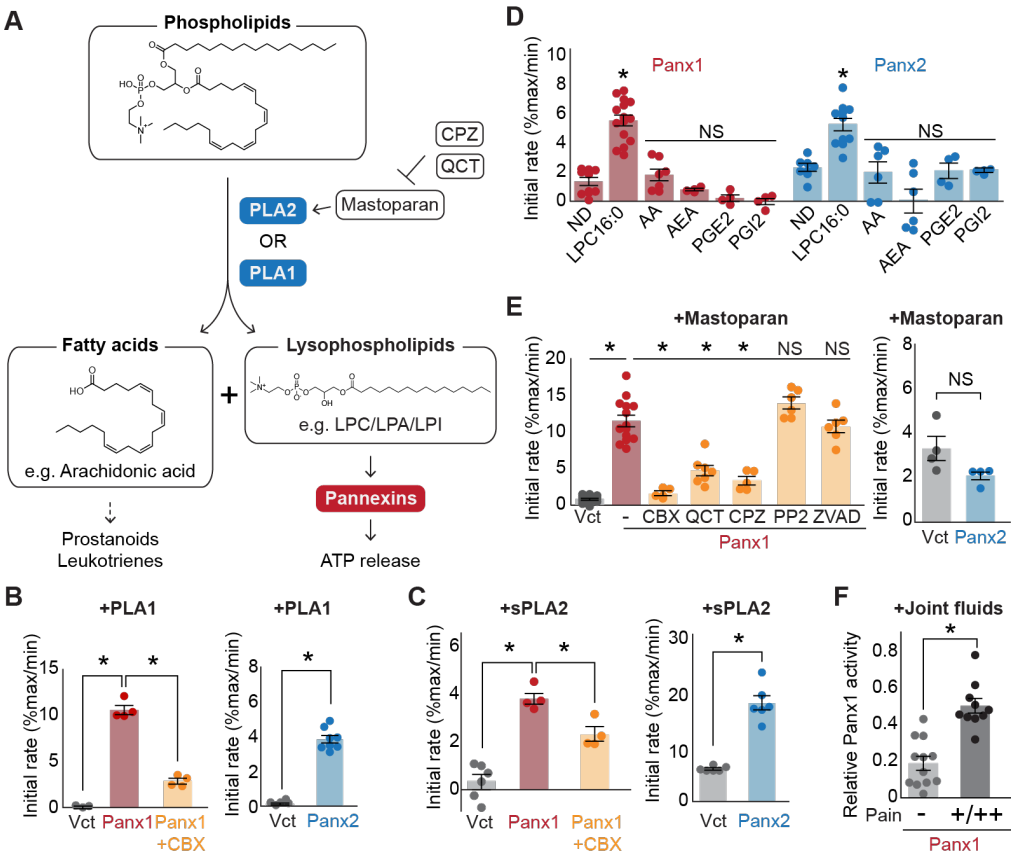

Fig. 4: Pannexins mediate lysophospholipid signaling. (**A**) Schematic illustrating lysophospholipid signaling. (**B**)-(**E**) Pannexin activities triggered by extracellularly applied stimuli. Normalized initial mVenus quenching rates are shown for PLA1 (B), sPLA2 (C), and major metabolic products of PLA2 (D), mastoparan with or without PLA2 inhibitors (QCT and CPZ), a Src kinase inhibitor (PP2), or a caspase inhibitor (ZVAD)(E). n=4-14. (**F**) Panx1-dependent mVenus quenching induced by synovial fluids obtained from canine patients with mild (-) or

moderate/severe (+/++) pain. The activity of each fraction was normalized to the effect of LPC-16:0 (30 μM). Each point represents a different patient. n=10-12. P values were calculated using unpaired Student's t-test with unequal variances ((B) and (C)) or using one-way ANOVA, followed by Dunnett's t-test ((D) and (E)). Asterisks indicate p<0.01. Error bars represent s.e.m.

LPC delocalizes the N-terminal domain for pannexin activation

How do lysophospholipids activate pannexin channels? To gauge where these pannexin activators bind, we performed molecular docking experiments. Blind docking of LPC16:0 to Panx1 (PDB ID: 7F8J)(*35*) uncovered that this molecule has the highest affinity to the hydrophobic pocket formed by transmembrane (TM)1, TM2, and N-terminal domain (NTD) between two neighboring protomers (Fig. 5A and B). We created six pairs of double asparagine (Asn) mutants in this pocket and tested whether decreasing hydrophobicity affects lysophospholipid-induced pannexin channel activation. While all Asn mutants retained voltage-induced channel activity, three Asn mutants (M37N/I41N, L48N/L52N, and L114N/I118N) nearly abolished the LPC16:0-induced currents (Fig. 5B and C, and Fig. S5). These data support that lysophospholipids likely bind to the pocket formed by TM1, TM2, and NTD through hydrophobic interactions.

To visualize the conformational changes triggered by lysophospholipids, we performed cryo-EM reconstruction of Panx1 and compared its conformations with or without these agonists. We used a biochemically stable version of the frog Panx1 construct that lacks the C-terminal 71 amino acids and 24 amino acids in the intracellular loop between transmembrane helices 2 and 3 (dubbed 'frPanx1-ΔLC')(*18*). We introduced the Gly and Ser insertion at the N-terminus (dubbed 'frPanx1-ΔLC+GS'), mimicking the cell-specific priming mechanism required for channel activation. Purified and liposome-reconstituted frPanx1-ΔLC+GS is activated by LPC16:0 in a dose-dependent manner (Fig. S4E-H), confirming that frPanx1-ΔLC+GS harbors the necessary activation machinery. To minimize potential interference of LPC activity by detergents, frPanx1-ΔLC+GS was reconstituted into lipid nanodiscs before cryo-EM grid preparation (Fig. S6 and S7).

We previously reported that the NTD of frPanx1-ΔLC extends into the intracellular space (Fig. 5D)(*18*). Here, we found that the C7-averaged map of frPanx1-ΔLC+GS in the absence of LPC16:0 showed conspicuous densities for the NTDs inside the central pore within the membrane boundary. Considering that the frPanx1-ΔLC+GS remains closed in the absence of LPC16:0, this dramatic flipping of the NTD may reflect Panx1 priming. Notably, addition of LPC16:0 to frPanx1-ΔLC+GS fragmented the NTD density inside the pore of the C7-averaged map, rendering the boundary between neighboring NTD densities unclear (Fig. 5D). The NTD remained fragmented in a low-pass filtered map at 3.4Å (Fig. S8A), confirming that this observation was not due to the slightly better resolution of the map with LPC16:0. In combination with the molecular docking and electrophysiology studies, it is likely that binding of LPC16:0 delocalizes the NTD to open the channel.

To gain further insight into the NTD delocalization triggered by LPC16:0, we isolated protomers from the heptameric channels using symmetry expansion followed by map subtraction. We used a mask covering one protomer including the area where the NTD density is visualized for frPanx1-ΔLC+GS (Fig. S8B). Three-dimensional classification of the protomer revealed that a major fraction (54%) of the untreated frPanx1-ΔLC+GS protomer ('primed' state) falls into one class (Class 6), in which a prominent NTD density is visible inside the pore (Fig. S8C). This is consistent with the strong NTD density observed in the C7-averaged map. Interestingly, Class 3 protomer showed that the NTD in this class sits near TM1 and 2 of the neighboring subunit, rather than its own TMs (Fig. S8E). While the weak EM density for the loop between the NTD and TM 1 in general indicates high flexibility in this region, it seems likely that at least a fraction of the NTDs prefer to be localized near the neighboring subunit. When the same mask was used to isolate the protomers of frPanx1-ΔLC+GS treated with LPC16:0 (activated state), 3D classification

resulted in much more heterogeneous and more evenly distributed subclasses (Fig. S8D). The most closely resembled class (Class 4) to the major class of the primed conformation (Class 6) contained only 8% of the total protomeric particles, suggesting a substantial rearrangement of the NTD. Several classes showed split densities in the NTD regions, which likely correspond to pieces of the two neighboring NTDs in the region (Fig. S8D). Such heterogeneous movement of the NTD likely contributed to the heavily fragmented NTD density in the C7-averaged map (Fig. 5D). Together, our study suggests that LPC16:0 opens the Panx1 channel by altering the conformation of the NTD in an uncoordinated manner.

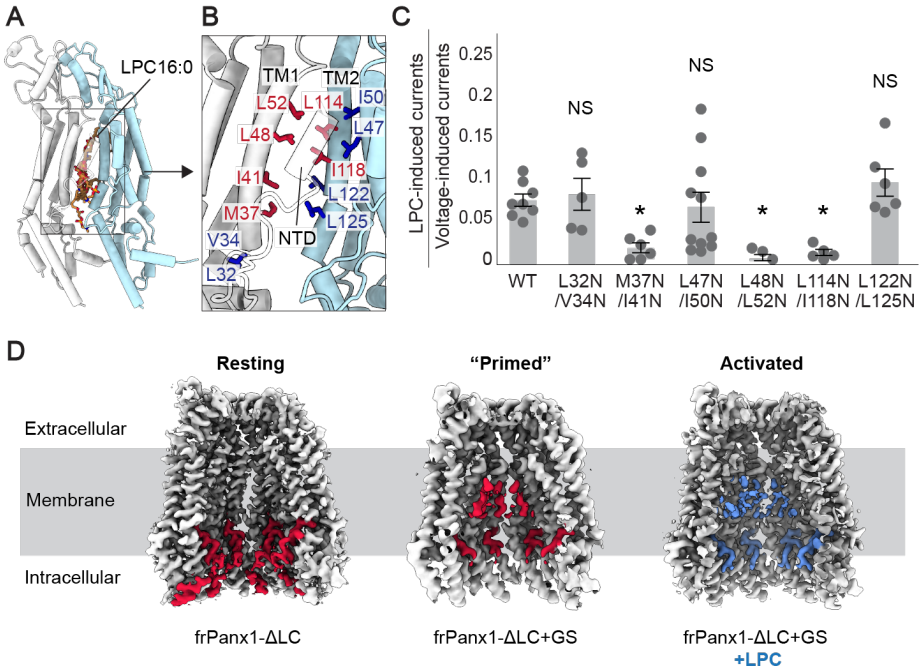

Fig. 5: LPC induces a conformational change in the N-terminal domain. (**A**) Molecular docking of LPC16:0 in the human Panx1 structure (PDB: 7F8J). Two protomers are used for the docking and superposition of the 10 most energetically favorable binding modes of LPC16:0 are shown as stick representations. (**B**) Close-up view of the predicted LPC16:0 binding pocket. Residues whose Asn mutations abolish LPC-induced currents are shown in red and those that preserve such currents are shown in blue. (**C**) Ratio of LPC-induced currents (7 μM) over voltage-induced currents (+110 mV) for the indicated double Asn mutants. Panx1+GS background was used for the whole-cell recordings from HEK cells. n=5-11. P values were calculated using one-way ANOVA followed by Dunnett's t-test. Asterisks denote $p<0.01$. Error bars represent s.e.m. (**D**) EM maps of Panx1 in its resting state (frPanx1-ΔLC (3.0 Å)), 'primed' state (frPanx1-ΔLC+GS (3.4 Å)), or activated state (frPanx1-ΔLC+GS+LPC (3.2 Å)). Each map represents only four of the seven protomers, for clarity. Map densities corresponding to the NTD are highlighted in red for the resting and primed states, or in blue for the activated state.

Discussion

In this study, we demonstrate that both Panx1 and Panx2 are directly and reversibly activated by lysophospholipids when applied at naturally occurring concentrations in body fluids or endogenously produced from the plasma phospholipids by PLA enzymes. This *bona fide* stimulus triggers ATP release from pannexin-expressing cells, uniting lipid and purinergic signaling pathways important for inflammation. Our *in vitro* reconstitution study demonstrates that full-length Panx1 can be activated by lysophospholipids in the absence of other proteins, providing

compelling evidence that this channel possesses an intrinsic mechanism for activation in this manner. Considering that lysophospholipid concentrations are elevated in many inflammatory diseases, pannexin-mediated ATP release likely plays a critical role in such pathological conditions. This is consistent with our experiments demonstrating that joint fluid from dogs experiencing pain triggers robust Panx1 activation.

The discovery of a common stimulus for Panx1 and Panx2 suggests partial functional overlap between these two subtypes. Indeed, compensatory roles between the two has been suggested in ischemic stroke (*54*) and insulin secretion from β-cells (*55*). Given that Panx3 is ~45% identical to Panx1 and shares a similar overall structure, it is surprising that Panx3 was not activated by lysophospholipids. Since Panx3 does not respond to lysophospholipids or elevated membrane potential even in GnTI$^-$ cells or with the addition of Gly and Ser at the N-terminus, this subtype may require a specific modification for proper priming or may respond to a different class of metabolites.

Our cryo-EM maps of frPanx1 suggest that pannexins undergo at least two major conformational changes for their activation, namely NTD flip and delocalization. Flipping of the NTD is supported by the recent cryo-EM structures of the human Panx1 channel, which demonstrate that an inhibitor traps the NTD into the intracellularly extended conformation, similar to the frPanx1-ΔLC (*35*). Since the NTD-flipped channel (e.g., frPanx1-ΔLC+GS) remains closed until lysophospholipids are applied, this drastic structural rearrangement may be a critical initial step to prime pannexin channels for stimulus-dependent opening. The many reported posttranslational modifications activating Panx1 may be explained by their ability to promote this upward NTD flip. Delocalization of the flipped NTD by lysophospholipids seems to occur heterogeneously, which is consistent with the quantized mechanism of pannexin activation (*15*). While we could not find obvious densities for LPC16:0 in our current maps probably due to a nonuniform mode of binding, both molecular docking and mutagenesis studies suggest that LPC16:0 binds in the hydrophobic pocket formed between the NTDs and TMs. Interestingly, a part of this LPC-binding pocket is occupied with a lipid molecule in some of the published Panx1 structures (*33, 35*). Given that a broad range of lysophospholipids can activate pannexins, we speculate that these agonists may function by replacing the pre-existing lipid molecules in this pocket, which in turn disrupts hydrophobic interactions between the NTDs and TMs.

Lysophospholipid-mediated pannexin activation makes biological sense for several reasons. First, PLA enzymes are activated by various receptors, such as NMDA, P2X7, TNF-α, and α1-adrenergic, which have been demonstrated to trigger pannexin channel opening (*26-28, 47, 56-59*). Second, recent study showed that LPC application triggers ATP release from macrophages (*60*). Third, the concentrations of lysophospholipids increase under pathological conditions, in which pannexins play significant roles. For example, vascular inflammation caused by platelet-derived microvesicles can be explained by the action of extracellular ATP released through Panx1 channels, as these microvesicles contain a large amount of LPCs (*61*). Likewise, potentiation of angiotensin-II dependent vasoconstriction by oxidized low-density lipoproteins (oxLDLs)—a condition associated with vasospasm in atherosclerotic arteries—may be mediated by Panx1 activation, since oxLDLs are rich in LPCs (*62*). In addition, both augmented Panx1 channel expression and elevated levels of lysophospholipids have been independently reported to be associated with insulin resistance (*39, 63*), a common health problem linked to a wide array of pathophysiologic conditions, including type 2 diabetes, hypertension, and atherosclerosis. Together, our study supports that pannexins are key downstream players in lysophospholipid signaling.

References and Notes

1. J. Linden, F. Koch-Nolte, G. Dahl, Purine Release, Metabolism, and Signaling in the Inflammatory Response. *Annu Rev Immunol* **37**, 325-347 (2019).
2. G. Burnstock, Purinergic nerves. *Pharmacological reviews* **24**, 509-581 (1972).
3. Z. Huang *et al.*, From purines to purinergic signalling: molecular functions and human diseases. *Signal Transduct Target Ther* **6**, 162 (2021).
4. S. Kinnamon, T. Finger, The Role of ATP and Purinergic Receptors in Taste Signaling. *Handb Exp Pharmacol* **275**, 91-107 (2022).
5. J. Sanderson *et al.*, Purines in the eye: recent evidence for the physiological and pathological role of purines in the RPE, retinal neurons, astrocytes, Muller cells, lens, trabecular meshwork, cornea and lacrimal gland. *Exp Eye Res* **127**, 270-279 (2014).
6. K. Inoue, The Role of ATP Receptors in Pain Signaling. *Neurochem Res* **47**, 2454-2468 (2022).
7. U. Schenk *et al.*, Purinergic control of T cell activation by ATP released through pannexin-1 hemichannels. *Sci Signal* **1**, ra6 (2008).
8. R. A. North, M. F. Jarvis, P2X receptors as drug targets. *Mol Pharmacol* **83**, 759-769 (2013).
9. H. Zimmermann, M. Zebisch, N. Strater, Cellular function and molecular structure of ecto-nucleotidases. *Purinergic Signal* **8**, 437-502 (2012).
10. J. Syrjanen, K. Michalski, T. Kawate, H. Furukawa, On the molecular nature of large-pore channels. *Journal of molecular biology*, 166994 (2021).
11. G. Dahl, ATP release through pannexon channels. *Philos Trans R Soc Lond B Biol Sci* **370**, (2015).
12. H. Imamura *et al.*, Single-cell dynamics of pannexin-1-facilitated programmed ATP loss during apoptosis. *eLife* **9**, (2020).
13. F. B. Chekeni *et al.*, Pannexin 1 channels mediate 'find-me' signal release and membrane permeability during apoptosis. *Nature* **467**, 863-867 (2010).
14. A. K. Narahari *et al.*, ATP and large signaling metabolites flux through caspase-activated Pannexin 1 channels. *eLife* **10**, (2021).
15. Y. H. Chiu *et al.*, A quantized mechanism for activation of pannexin channels. *Nature communications* **8**, 14324 (2017).
16. J. K. Sandilos *et al.*, Pannexin 1, an ATP release channel, is activated by caspase cleavage of its pore-associated C-terminal autoinhibitory region. *J Biol Chem* **287**, 11303-11311 (2012).
17. X. Jin *et al.*, A Constitutively Closed Pannexin1 Channel in Lipid Bilayer Nanodiscs Assembles as a Large-Pore Heptamer. *bioRxiv*, (2021).
18. K. Michalski *et al.*, The cryo-EM structure of a pannexin 1 reveals unique motifs for ion selection and inhibition. *eLife* **9**, (2020).
19. M. S. Aquilino, P. Whyte-Fagundes, G. Zoidl, P. L. Carlen, Pannexin-1 channels in epilepsy. *Neurosci Lett* **695**, 71-75 (2019).
20. M. F. Munoz, T. N. Griffith, J. E. Contreras, Mechanisms of ATP release in pain: role of pannexin and connexin channels. *Purinergic Signal* **17**, 549-561 (2021).
21. A. K. Yeung, C. S. Patil, M. F. Jackson, Pannexin-1 in the CNS: Emerging concepts in health and disease. *J Neurochem* **154**, 468-485 (2020).
22. P. A. Harcha, T. Lopez-Lopez, A. G. Palacios, P. J. Saez, Pannexin Channel Regulation of Cell Migration: Focus on Immune Cells. *Front Immunol* **12**, 750480 (2021).
23. S. E. Adamson *et al.*, Pannexin 1 is required for full activation of insulin-stimulated glucose uptake in adipocytes. *Mol Metab* **4**, 610-618 (2015).
24. V. R. Lee *et al.*, Pannexin 1 regulates adipose stromal cell differentiation and fat accumulation. *Sci Rep* **8**, 16166 (2018).

25. M. Koval, W. J. Schug, B. E. Isakson, Pharmacology of pannexin channels. *Curr Opin Pharmacol* **69**, 102359 (2023).
26. M. Billaud *et al.*, Pannexin1 regulates alpha1-adrenergic receptor- mediated vasoconstriction. *Circ Res* **109**, 80-85 (2011).
27. R. J. Thompson *et al.*, Activation of pannexin-1 hemichannels augments aberrant bursting in the hippocampus. *Science* **322**, 1555-1559 (2008).
28. D. Maier-Begandt *et al.*, A venous-specific purinergic signaling cascade initiated by Pannexin 1 regulates TNFalpha-induced increases in endothelial permeability. *Sci Signal* **14**, (2021).
29. L. J. DeLalio *et al.*, Constitutive SRC-mediated phosphorylation of pannexin 1 at tyrosine 198 occurs at the plasma membrane. *J Biol Chem* **294**, 6940-6956 (2019).
30. Y. H. Chiu *et al.*, Deacetylation as a receptor-regulated direct activation switch for pannexin channels. *Nature communications* **12**, 4482 (2021).
31. Y. H. Chiu, M. S. Schappe, B. N. Desai, D. A. Bayliss, Revisiting multimodal activation and channel properties of Pannexin 1. *J Gen Physiol* **150**, 19-39 (2018).
32. C. Ambrosi *et al.*, Pannexin1 and Pannexin2 channels show quaternary similarities to connexons and different oligomerization numbers from each other. *J Biol Chem* **285**, 24420-24431 (2010).
33. Z. Ruan, I. J. Orozco, J. Du, W. Lu, Structures of human pannexin 1 reveal ion pathways and mechanism of gating. *Nature* **584**, 646-651 (2020).
34. Z. Deng *et al.*, Cryo-EM structures of the ATP release channel pannexin 1. *bioRxiv*, (2020).
35. M. Kuzuya *et al.*, Structures of human pannexin-1 in nanodiscs reveal gating mediated by dynamic movement of the N terminus and phospholipids. *Sci Signal* **15**, eabg6941 (2022).
36. K. Michalski, T. Kawate, Carbenoxolone inhibits Pannexin1 channels through interactions in the first extracellular loop. *J Gen Physiol* **147**, 165-174 (2016).
37. Z. Liu *et al.*, Predator-secreted sulfolipids induce defensive responses in C. elegans. *Nature communications* **9**, 1128 (2018).
38. K. Michalski, E. Henze, P. Nguyen, P. Lynch, T. Kawate, The weak voltage dependence of pannexin 1 channels can be tuned by N-terminal modifications. *J Gen Physiol* **150**, 1758-1768 (2018).
39. S. H. Law *et al.*, An Updated Review of Lysophosphatidylcholine Metabolism in Human Diseases. *Int J Mol Sci* **20**, (2019).
40. S. T. Tan, T. Ramesh, X. R. Toh, L. N. Nguyen, Emerging roles of lysophospholipids in health and disease. *Prog Lipid Res* **80**, 101068 (2020).
41. I. K. Poon *et al.*, Unexpected link between an antibiotic, pannexin channels and apoptosis. *Nature* **507**, 329-334 (2014).
42. P. J. Reeves, N. Callewaert, R. Contreras, H. G. Khorana, Structure and function in rhodopsin: high-level expression of rhodopsin with restricted and homogeneous N-glycosylation by a tetracycline-inducible N-acetylglucosaminyltransferase I-negative HEK293S stable mammalian cell line. *Proc Natl Acad Sci U S A* **99**, 13419-13424 (2002).
43. T. Nagai *et al.*, A variant of yellow fluorescent protein with fast and efficient maturation for cell-biological applications. *Nat Biotechnol* **20**, 87-90 (2002).
44. L. J. Galietta, P. M. Haggie, A. S. Verkman, Green fluorescent protein-based halide indicators with improved chloride and iodide affinities. *FEBS Lett* **499**, 220-224 (2001).
45. S. Marra *et al.*, Non-acidic activation of pain-related Acid-Sensing Ion Channel 3 by lipids. *Embo J* **35**, 414-428 (2016).
46. F. Maingret, A. J. Patel, F. Lesage, M. Lazdunski, E. Honore, Lysophospholipids open the two-pore domain mechano-gated K(+) channels TREK-1 and TRAAK. *J Biol Chem* **275**, 10128-10133 (2000).

47. P. Pelegrin, A. Surprenant, Pannexin-1 mediates large pore formation and interleukin-1beta release by the ATP-gated P2X7 receptor. *Embo J* **25**, 5071-5082 (2006).
48. A. M. Vasquez, V. D. Mouchlis, E. A. Dennis, Review of four major distinct types of human phospholipase A2. *Adv Biol Regul* **67**, 212-218 (2018).
49. M. Dosch, J. Gerber, F. Jebbawi, G. Beldi, Mechanisms of ATP Release by Inflammatory Cells. *Int J Mol Sci* **19**, (2018).
50. E. A. Dennis, P. C. Norris, Eicosanoid storm in infection and inflammation. *Nat Rev Immunol* **15**, 511-523 (2015).
51. M. Joyce-Brady *et al.*, Mechanisms of mastoparan-stimulated surfactant secretion from isolated pulmonary alveolar type 2 cells. *J Biol Chem* **266**, 6859-6865 (1991).
52. J. Gil, T. Higgins, E. Rozengurt, Mastoparan, a novel mitogen for Swiss 3T3 cells, stimulates pertussis toxin-sensitive arachidonic acid release without inositol phosphate accumulation. *J Cell Biol* **113**, 943-950 (1991).
53. F. Jacquot *et al.*, Lysophosphatidylcholine 16:0 mediates chronic joint pain associated to rheumatic diseases through acid-sensing ion channel 3. *Pain* **163**, 1999-2013 (2022).
54. P. Bargiotas *et al.*, Pannexins in ischemia-induced neurodegeneration. *Proc Natl Acad Sci U S A* **108**, 20772-20777 (2011).
55. L. A. Berchtold *et al.*, Pannexin-2-deficiency sensitizes pancreatic beta-cells to cytokine-induced apoptosis in vitro and impairs glucose tolerance in vivo. *Mol Cell Endocrinol* **448**, 108-121 (2017).
56. R. M. Burch, A. Luini, J. Axelrod, Phospholipase A2 and phospholipase C are activated by distinct GTP-binding proteins in response to alpha 1-adrenergic stimulation in FRTL5 thyroid cells. *Proc Natl Acad Sci U S A* **83**, 7201-7205 (1986).
57. E. Alzola *et al.*, Activation by P2X7 agonists of two phospholipases A2 (PLA2) in ductal cells of rat submandibular gland. Coupling of the calcium-independent PLA2 with kallikrein secretion. *J Biol Chem* **273**, 30208-30217 (1998).
58. L. Tapia-Arancibia, F. Rage, M. Recasens, J. P. Pin, NMDA receptor activation stimulates phospholipase A2 and somatostatin release from rat cortical neurons in primary cultures. *Eur J Pharmacol* **225**, 253-262 (1992).
59. W. G. Hoeck, C. S. Ramesha, D. J. Chang, N. Fan, R. A. Heller, Cytoplasmic phospholipase A2 activity and gene expression are stimulated by tumor necrosis factor: dexamethasone blocks the induced synthesis. *Proc Natl Acad Sci U S A* **90**, 4475-4479 (1993).
60. S. Ismaeel, A. Qadri, ATP Release Drives Inflammation with Lysophosphatidylcholine. *Immunohorizons* **5**, 219-233 (2021).
61. P. Diehl *et al.*, Lysophosphatidylcholine is a Major Component of Platelet Microvesicles Promoting Platelet Activation and Reporting Atherosclerotic Plaque Instability. *Thromb Haemost* **119**, 1295-1310 (2019).
62. J. Galle *et al.*, Oxidized LDL and its compound lysophosphatidylcholine potentiate AngII-induced vasoconstriction by stimulation of RhoA. *J Am Soc Nephrol* **14**, 1471-1479 (2003).
63. M. Tozzi, J. B. Hansen, I. Novak, Pannexin-1 mediated ATP release in adipocytes is sensitive to glucose and insulin and modulates lipolysis and macrophage migration. *Acta Physiol (Oxf)* **228**, e13360 (2020).
64. T. K. Ritchie *et al.*, Chapter 11 - Reconstitution of membrane proteins in phospholipid bilayer nanodiscs. *Methods in enzymology* **464**, 211-231 (2009).
65. J. Zivanov *et al.*, A Bayesian approach to single-particle electron cryo-tomography in RELION-4.0. *eLife* **11**, (2022).
66. S. Q. Zheng *et al.*, MotionCor2: anisotropic correction of beam-induced motion for improved cryo-electron microscopy. *Nat Methods* **14**, 331-332 (2017).
67. A. Rohou, N. Grigorieff, CTFFIND4: Fast and accurate defocus estimation from electron micrographs. *J Struct Biol* **192**, 216-221 (2015).

68. Y. Z. Tan *et al.*, Addressing preferred specimen orientation in single-particle cryo-EM through tilting. *Nat Methods* **14**, 793-796 (2017).

Acknowledgments: We thank O. Boudker, K. Swartz, J. Davis, A. Alouani, and the members of the Fromme and the Kawate labs for helpful discussions; W. Greentree and M. Linder for providing mouse tissues; M. Silvestry Ramos, K. Spoth, J. Kaminsky, G. Hu, and L. Wang, for support on cryo-EM data collection; S. Webb for the help on joint fluid sample collection. This work made use of the Cornell Center for Materials Research Shared Facilities which are supported through the NSF MRSEC program (DMR-1719875). The Laboratory for BioMolecular Structure (LBMS) is supported by the DOE Office of Biological and Environmental Research (KP1607011)

Funding:

National Institutes of Health grant R01GM114379 (EH, TK)

National Institutes of Health grant R35GM131877 (FCS)

National Institutes of Health grant T32GM008267 (KM)

National Science Foundation grant DBI1659534 (LK)

National Science Foundation grant 2222495 (JJE)

Human Frontier Science Program grant RGY0075 (JJE)

Cornell Margaret and Richard Riney Canine Health Center Research Grants Program (EH, JMB, TK)

Author contributions:

Conceptualization: EH, TK

Methodology: EH, JJE, RNB, BWF, JMB, FCS, TK

Investigation: EH, JJE, RNB, BWF, KM, LK, ML, JMB

Visualization: EH, JJE, BWF, TK

Funding acquisition: JMB, FCS, TK

Project administration: JMB, FCS, TK

Supervision: JMB, FCS, TK

Writing – original draft: EH, TK

Writing – review & editing: EH, JJE, BWF, KM, JMB, FCS, TK

Competing interests: Authors declare that they have no competing interests

Supplementary Materials

Materials and Methods

Figs. S1 to S8

References (#64-68)